Dielectric response analysis of a conducting polymer dominated by the hopping charge transport

1998 J. Phys.: Condens. Matter 10 5595

(http://iopscience.iop.org/0953-8984/10/25/011)

J. Phys.: Condens. Matter **10** (1998) 5595–5617. Printed in the UK PII: S0953-8984(98)87683-2

Dielectric response analysis of a conducting polymer dominated by the hopping charge transport

S Capaccioli†‡, M Lucchesi†, P A Rolla† and G Ruggeri§

† INFM and Physics Department, University of Pisa, piazza Torricelli 2, 56126 Pisa, Italy

‡ Department of Chemical Engineering, Industrial Chemistry and Materials Science, University of Pisa, Italy

§ Department of Chemistry and Industrial Chemistry, University of Pisa, via Risorgimento 35, 56126 Pisa, Italy

Received 17 September 1997, in final form 26 March 1998

Abstract. The d.c. conductivity and the electric a.c. response from 100 Hz up to 40 MHz of poly(3*n*-decylpyrrole) were measured in the 80–330 K interval to characterize the charge transport behaviour of the system. The d.c. conductivity well fitted the variable range hopping model, and the loss factor, after having deducted the d.c. contribution, showed a relaxation peak when the conductivity versus frequency started to rise. The strength of this relaxation increased with temperature and became too large to be related to a dipolar relaxation; moreover, the temperature dependence of the loss peak frequency and d.c. conductivity coincided. The observed relaxation was attributed to the hopping charge transport, as further confirmed by the temperature behaviour of the relaxation strength and by the frequency dependence of the exponents of the power law which locally approximate the conductivity behaviour. As the activation energy of the d.c. conductivity differed from the frequency of the loss peak, the theoretical prediction concerning the selfsimilarity of the a.c. conductivity was roughly verified.

1. Introduction

Polymeric materials which are intrinsically conductive have very attractive features for many electronic applications; unfortunately the highest conductivities are generally accompanied by relatively poor processability and chemical stability. The search for a right compromise requires a better understanding of the charge transport mechanisms which are involved, besides a deeper knowledge of the structure–property relationships. In this paper we deal with the electrical transport properties of poly(3*n*-decylpyrrole) (P3DP) [1], having a moderate conductivity but a promising chemical stability and processability.

Although until now many accurate experiments were carried out [2, 3], the mechanism of charge transport in conducting polymers has yet to be clarified in detail. The conductivity is achieved by doping, which produces the formation of solitons [4–6], or polarons and bipolarons [7] along the conjugated chain. The counterions, injected by doping, remain close to the conjugation defects, thus granting the electrical neutrality of each macromolecule. Some peculiar conduction mechanisms [8, 9], related to the motion of charge carriers delocalized along the macromolecular chains, can be supposed; however, in most common conducting polymers (e.g. pyrrole and thiophene derivative polymers), owing to the doping inhomogeneity and structural disorder (crosslinks, dead ends etc) [10] that limits the conjugation length, the d.c. conductivity is usually modelled by a phonon-assisted hopping

0953-8984/98/255595+23$19.50

of electrons between randomly distributed localized states [11]. The transport process is dominated by the macroscopic disorder rather than by the characteristic properties of the conjugation defects. On the other hand, the charge transport mechanism is effective not only on the macromolecular backbone (intra-chain hopping) but also between different macromolecules (inter-chain hopping) [12, 13]. The charge transfer mechanism which is the origin of the d.c. conductivity of these systems can be explained by the 3D hopping among localized states, as typically occurs in some amorphous semiconductors [14], or even by the hopping among metallic-like regions separated by insulating barriers, as in cermets [15]. In some highly conducting polymers, an insulator–metal transition (IMT) was found [16, 17]. While in the insulating regime the temperature-dependent d.c conductivity and the electric a.c. response were well described by the hopping models, different behaviours were found near and beyond the IMT boundary [18].

In general, the a.c. electric response becomes a superposition of different contributions: the dielectric response of the bound charges (dipolar response) sums up to the hopping of the localized charge carriers and to the response produced by the deformation of the molecular structures following the diffusion of charge carriers along a percolation path. The overall electric behaviour can be suitably studied by means of the generalized complex dielectric permittivity [19], as it takes into account both conductivity and dielectric polarization. This quantity can be measured by means of the impedance spectroscopy technique, which provides both d.c. and a.c. behaviour. In these experiments the main issue is the correct assignment of the observed behaviour to the various phenomena which occur in the system; besides the conductivity and dipolar polarization, there are electrode effects, interfacial effects and space charge relaxations. The correct interpretation of the experiments is obtained by verifying the reliability and physical grounding of the model by which the fitting procedure is carried out.

2. Theoretical and phenomenological aspects

Many theories provide a description of the behaviour of the conductivity in disordered systems dominated by hopping conduction, when both temperature of the system and frequency of the applied electric field are varied [20].

The dependence on temperature T of the d.c. conductivity can be conveniently represented by the Mott law [21]:

$$\sigma_{dc}(T) = \frac{A}{T^b} \exp\left(-\left(\frac{T_0}{T}\right)^{\gamma}\right) = \sigma_0 \exp\left(-\left(\frac{T_0}{T}\right)^{\gamma}\right) \tag{1}$$

based on 3D fixed ($\gamma = 1$) or variable ($\gamma < 1$) range hopping (VRH) models. The constants A and T_0 depend on the localization and density of the states; the exponents b and γ depend on the distribution of states around the Fermi level; the value of γ, in particular, is related to the dimensions of the transport process. In three dimensions usual values of γ are $1/2$ and $1/4$. The value $\gamma = 1/2$ is probably determined by a Coulomb-type electron–electron correlation, which leads to a weak gap near the Fermi level, the so-called Coulomb gap [22, 23], and to a square dependence of the localized state density on the energy. For $\gamma = 1/4$, the density of localized states near the Fermi level does not depend on energy [20]. Like γ, the exponent b, which affects the temperature dependence of the pre-exponential factor σ_0, is determined by the localized state distribution near the Fermi level. If the state density depends on the square of the energy, $b = -1$ and $\sigma_0(T)$ linearly rises with temperature; otherwise, if the state density is constant, $b = 1/2$ [20].

Equation (1) was also confirmed by both the percolation theory [24] and computer simulations [25], and it was experimentally verified in a wide variety of materials [21]. According to Mott, a charge carrier hops from the localized i- to the j-state at the transition rate W_{ij}

$$W_{ij} = \nu_0 \exp(-2\alpha R_{ij} - \Delta E_{ij}/k_B T) \tag{2}$$

where α is the reciprocal state localization amplitude, R_{ij} is the hopping distance, ΔE_{ij} the energy difference between the two states, k_B is the Boltzmann constant and ν_0 represents the number of hop attempts per unit of time, which is of the order of magnitude of the optical phonon frequency. The VRH model accounts for the considerable contribution at low temperature of the charge carriers jumping to not neighbour, but energetically favourable, states. A key quantity of the hopping mechanism is the critical rate W_c, i.e. the fastest rate at which a macroscopic continuous path across the material can exist; such a path should be made by all the i–j pairs of states with a transition rate $W_{ij} > W_c$ [24, 26]. The rate W_c determines the d.c. conductivity value; in particular, σ_{dc} and W_c are proportional and show the same temperature dependence.

The response of a conducting material to an a.c. electric field can be described by the complex conductivity, $\sigma^*(\omega) = \sigma'(\omega) + \mathrm{i}\sigma''(\omega)$, and by the complex permittivity, $\varepsilon^*(\omega) = \varepsilon'(\omega) - \mathrm{i}\varepsilon''(\omega)$. In fact, these quantities are related by the following equations:

$$\varepsilon'(\omega) - \varepsilon_\infty = \frac{\sigma''(\omega)}{\varepsilon_0 \omega} \qquad \varepsilon''(\omega) = \frac{\sigma'(\omega)}{\varepsilon_0 \omega} = \varepsilon_d'' + \frac{\sigma_{dc}}{\varepsilon_0 \omega} \qquad \varepsilon_d''(\omega) = \frac{\sigma'(\omega) - \sigma_{dc}}{\varepsilon_0 \omega} \tag{3}$$

where ω is the angular frequency, ε_∞ is the unrelaxed dielectric constant, ε_0 is the vacuum permittivity and $\varepsilon_d''(\omega)$ is the imaginary part of the permittivity after deducting the conductivity contribution. In a disordered system where the hopping mechanism dominates, the conductivity increases as the frequency of the electric field is increased, because the contribution of charge carriers moving along smaller and smaller distances, i.e., confined inside clusters of progressively decreasing sizes, increases [27]. As the real and imaginary parts of the complex conductivity are related to each other by the Kramers–Kronig relations and to complex permittivity by (3), this effect modifies the overall electric response of the system to the driving electric field.

Several theories were developed to describe the frequency dependence of the electric response of a system where the hopping transport mechanism dominates. The total a.c. response in the high-frequency limit was described by the pair approximation (PA) introduced by Pollak and Geballe [28]. They assumed a total response produced by the sum of the individual responses of pairs of sites randomly distributed throughout the material. Moreover, any contribution to the conductivity from clusters of more than two sites was completely neglected (in a period of applied field the carriers can hop only between two sites), and the infinite cluster case (i.e., the case of d.c. conductivity) was separately treated. In the pair approximation theory the complex conductivity obeys a fractional power law: $\sigma'(\omega) \propto \omega^{s'}$ and $\sigma''(\omega) \propto \omega^{s''}$, with both s' and s'' less than 1 ($s' > s''$), and slightly increasing with the frequency.

At intermediate frequencies, in a period of the applied electric field, the carriers can cross a number of sites (multiple hopping region). The theoretical approaches developed for this case can be roughly classified in two groups, referred as the *effective-medium* and *cluster* theories, respectively. The theories of the first group, which include the *effective-medium approximation* (EMA) model [29], the *extended pair approximation* (EPA) model [30, 31, 32] and the *coherent medium approximation* (CMA) model [33], represent the disordered medium surrounding a particular pair of sites by an effective ordered medium,

whose parameters are subsequently chosen to match the properties of the actual medium. The theories of the second group, such as the *continuous-time random-walk* model [34] or the *percolation-path approximation* (PPA) [35], solve directly the frequency dependent percolation problem using the transition probability distribution among sites.

All the models for the intermediate frequency region consider the d.c. and a.c. conductivities as originating from the same hopping mechanism [36]. In this approach, the conductivity of a 3D system with a density n of charge carriers follows from the Einstein relation [34]:

$$\sigma^*(\omega) = \sigma'(\omega) + \mathrm{i}\sigma''(\omega) = \frac{ne^2}{k_B T} D(\omega) \tag{4}$$

where e is the electron charge. $D(\omega)$ is the a.c. diffusion constant defined as:

$$D(\omega) = W^*(\omega) R_{op}^2 \tag{5}$$

where $W^*(\omega)$ and R_{op} are the optimal coherent hopping rate and the characteristic hopping length, respectively. For $\omega = 0$, (4) provides the equation of the d.c. diffusion:

$$\sigma_{dc} = \frac{ne^2}{k_B T} R_{op}^2 W_c. \tag{6}$$

The quantities W_c and R_{op} can be related to the parameters σ_0 and T_0 in (1) by the following relationships [20]:

$$W_c = \nu_0 \exp\left(-\left(\frac{T_0}{T}\right)^{\gamma}\right) \qquad \sigma_0 = \frac{ne^2}{k_B T} R_{op}^2 \nu_0. \tag{7}$$

By combining (4), (5), (6) and (7), you can define a normalized complex conductivity σ_n^* in terms of the optimal coherent hopping rate:

$$\sigma_n^*(\omega, T) = \sigma_n' + \mathrm{i}\sigma_n'' = \frac{\sigma^*(\omega, T)}{\sigma_{dc}(T)} = \frac{W^*(\omega, T)}{W_c(T)}. \tag{8}$$

In the multiple hopping region, i.e., for frequencies below the real part W' of the optimal coherent hopping rate W^*, the complex conductivity σ_n^* shows a selfsimilar behaviour if plotted versus the dimensionless frequency, Ω, defined by the following relation:

$$\Omega = \omega/\omega_c = \omega k / W_c. \tag{9}$$

ω_c is a characteristic frequency proportional to the hopping critical rate W_c through the constant k which depends on the material [37]; ω_c defines a frequency scale for the electric response of the overall system.

All the models EMA, EPA, PPA and CMA lead to similar behaviours of the normalized conductivity $\sigma_n^*(\Omega)$; the common characteristics are:

- The frequency dispersion of the conductivity occurs at about the frequency $\Omega = 1$.
- In the extremely low frequency region, i.e., for $\Omega = \omega/\omega_c \ll 1$, the conductivity can be written [20, 29–32, 36, 38]:

$$\sigma_n^*(\Omega) - 1 = \mathrm{i}\alpha_1 \Omega + \alpha_2 \Omega^2 \tag{10}$$

where α_1 and α_2 are constants depending on the model.

- At higher frequencies, i.e. for $1 \ll \Omega < W'/\omega_c$, all the theories predict for both σ_n' and σ_n'' a rising trend which is approximately represented by a power law: $\sigma_n' \propto \Omega^{s'}$, $\sigma_n'' \propto \Omega^{s''}$ (both s' and s'' lower than 1).

According to (10), the imaginary part of the normalized conductivity linearly depends on the frequency, then from (3) it follows that $\varepsilon'(\omega, T)$ is frequency independent, i.e., coincides with the static value ε_s given by the following equation:

$$\varepsilon_s - \varepsilon_\infty = \frac{\sigma_{dc}}{W_c}\frac{\alpha_1 k}{\varepsilon_0}. \tag{11}$$

The real part of (10) has a square dependence on frequency, then $\varepsilon''_d(\Omega)$ goes linearly to zero for $\Omega \ll 1$. Moreover, as $\sigma'_n/\Omega \propto \Omega^{s'-1}$, $\varepsilon''_d(\Omega)$ zeros even for $\Omega \gg 1$. Consequently, a loss peak for $\varepsilon''_d(\Omega)$ is expected to occur in the intermediate region, where the real part $\varepsilon'(\Omega)$ decreases from ε_s according to the power law behaviour $\Omega^{(1-s'')}$ [36]; the slope of $\varepsilon''_d(\Omega)$ is expected to come near 2 below the loss peak frequency and to approach $s'-1$ above the peak frequency. This result means that the electric response produced by the hopping mechanism in the intermediate frequency region can be described in a quite similar way as for the dipolar polarization, the dielectric parameters having a different meaning and temperature behaviour. In fact, when the electric response is dominated by the charge hopping transport, the characteristic parameters, as well as the relaxation strength $\Delta\varepsilon = \varepsilon_s - \varepsilon_\infty$, the critical frequency ω_c and the frequency of maximum of the loss peak ω_m, are affected by the d.c. conductivity. This can be shown by substituting in (11) σ_{dc} obtained from (6) and (7):

$$\Delta\varepsilon = \sigma_0(T)\frac{\alpha_1 k}{\nu_0 \varepsilon_0}. \tag{12}$$

The relaxation strength, $\Delta\varepsilon$, shows the same dependence on temperature as the pre-exponential factor $\sigma_0(T)$ which influences the d.c. conductivity behaviour in (1). Similarly, the critical frequency ω_c, defined by (9), can be rewritten by means of (6), (7), (9) and (11) in the form

$$\omega_c = \frac{W_c}{k} = \frac{\sigma_{dc}(T)\alpha_1}{\Delta\varepsilon(T)\,\varepsilon_0} = \frac{\nu_0}{k}\,\exp\left(-\left(\frac{T_0}{T}\right)^{\gamma}\right). \tag{13}$$

This last shows that ω_c has the same temperature dependence as the exponential factor of the d.c. conductivity in (1).

Finally, as the electric response is selfsimilar if plotted versus $\Omega = \omega/\omega_c$, the loss peak ω_m shifts with temperature as the critical frequency ω_c. Then, the condition $\omega_m \propto \omega_c$ can be rewritten by means of (13) leading to the relationship:

$$\sigma_{dc} = p\Delta\varepsilon\varepsilon_0\omega_m \tag{14}$$

which is called the Barton–Nakajima–Namikawa (BNN) condition [39–41]. As the parameter p is temperature independent and of the order of 1, (14) demonstrates that the frequency position of the loss peak is determined by the d.c. conductivity. The main difficulty of the analysis of electric response is distinguishing between polarization and conductivity effects. To give an idea of this difficulty, let us consider three different electric response functions: a typical dipolar response, i.e., the normalized Havriliak–Negami relaxation function (HN) with respect to the normalized variable $\Omega = \omega\tau$ (τ is the relaxation time) [42], $H(\Omega) = [1 + (\mathrm{i}\Omega)^{1-\alpha}]^{-\beta}$; the response function predicted by the hopping model based on the effective medium approximation (EMA) and that predicted by the model based on percolation path approximation (PPA). These functions were compared by calculating the real and imaginary parts of the normalized conductivity (8) under the following conditions: for the dipolar response, the values $\alpha = 0$ and $\beta = 0.7$ for the HN parameters were assumed, and the normalized conductivity was written as $\sigma_n^* = 1 + H(\Omega)\Omega$ by taking into account (3), (8), (9) and (11); for the EMA model,

the equation $W(\Omega)^*/W_c = \exp[i\Omega W/W^*(\Omega)]$ was numerically solved and the normalized conductivity was calculated by (8) [20]; for PPA, the Dyre function, $\sigma_n^* = i\Omega/\log_e(1+i\Omega)$, was considered [27, 35].

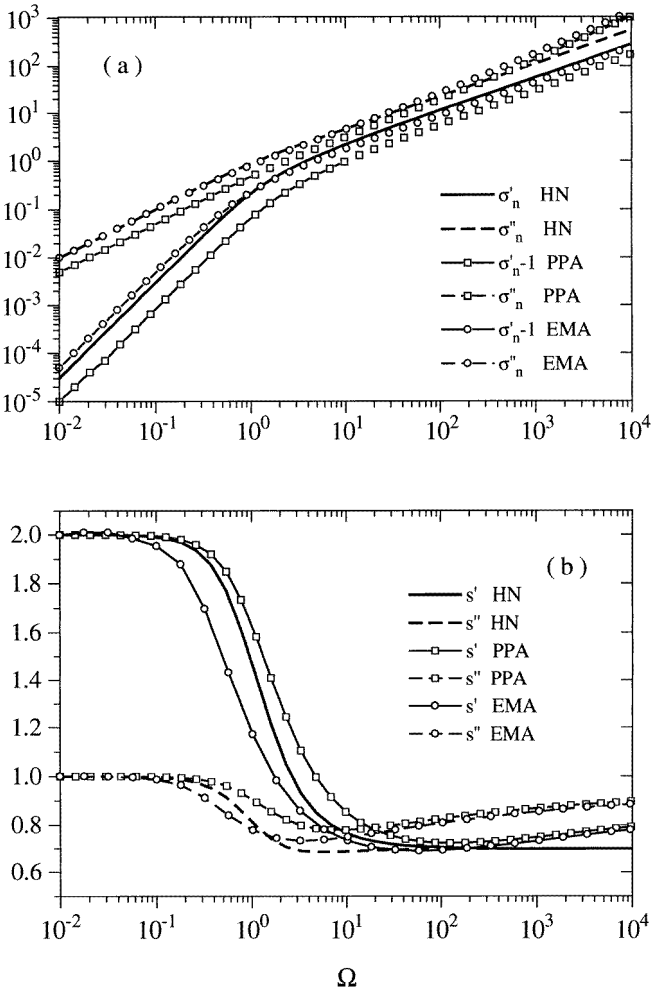

Figure 1. (a) Plot of $(\sigma_n' - 1)$ and σ_n'' against Ω for various response functions (see text). (b) Plot of the log derivatives s' and s'' of the corresponding functions in (a). In the case of the HN function, s' and s'' become equal and frequency independent at high Ω.

As the trends of all the functions (figure 1(a)) are very similar, very accurate experimental data, together with a carefully analysis of the additional peculiarities, are needed to show which function is more suitable to represent the behaviour of a given system. A more sensitive method for a such assignment can be applied if the experimental data have a sufficient accuracy to calculate the s' and s'' exponents from the logarithmic derivatives of the functions, $(\sigma_n' - 1)$ and σ_n'', which are defined by the following equations:

$$s'(\Omega) = \frac{\partial}{\partial \log_e(\Omega)} \log_e(\sigma_n' - 1) \tag{15a}$$

$$s''(\Omega) = \frac{\partial}{\partial \log_e(\Omega)} \log_e \sigma_n''. \tag{15b}$$

These quantities calculated for the functions of figure 1(a) and drawn in figure 1(b), are able to point out some differences among various models which could not be recognized by simply plotting the normalized conductivity.

All the theoretical models here mentioned were developed to explain some of the typical behaviours which have been recognized in the electrical response of disordered solids. In fact, the experiments showed that the peak of the quantity $\varepsilon_d''(\omega)$ (3) is broad and asymmetric, and then markedly different from a Debye-like relaxation peak [27, 36, 43, 44].

The shape of such a loss peak, normalized to the peak amplitude, is temperature independent. Moreover, the real part of the conductivity decreases and gradually becomes stable on approaching the low frequencies; the rising edge occurs around the frequency of the loss peak.

It was also observed that σ_{dc} and ω_m depend on temperature according to the Arrhenius law, and the activation energy is the same (more complex temperature dependences were also observed) [36]. Finally, in ionic and electronic glasses it was found that the BNN relationship (14) between frequency ω_m of the loss peak and σ_{dc} is fulfilled [41, 45, 46].

However, as all the models account for these experimental characteristics, the predicted behaviour of the electric response does not greatly differ from a hopping model to another; on the other hand, the peculiar characteristics of the materials are not sufficiently considered. Consequently, a precise experimental verification of a specific model is often impossible, and then the elements previously recalled are generally expected as more useful to distinguish between conductivity and dipolar relaxation.

In any case, even if the analysis of experimental data fails the objective to decide which model is more appropriate to represent the conductivity behaviour, it can eventually provide results capable of giving a rationale of the observed phenomena, provided that all the different phenomenological aspects are examined and compared. Accordingly, we have approached the discussion of our experimental results in the next sections by taking into account all the phenomenological aspects of the electric response of our system before checking a specific model. That allowed us to assign the observed relaxation to the charge hopping process, which is the most probable cause of the d.c. and a.c. conductivity in our system.

3. Experiment

3.1. Materials

Poly(3*n*-decylpyrrole) (P3DP) is a pyrrole derivative where the hydrogen atom in position 3 was substituted with a long alkylic chain (figure 2). The molecular structure of poly(3*n*-decylpyrrole) is planar with a centre of symmetry; Raman and IR spectroscopy measurements [47] have shown that, like in polypyrrole [48, 49], adjacent pyrrole rings in P3DP are oriented in opposite directions. The alkylic side chains can be shaped as random coils and x-ray experiments [50] did not find any supramolecular order.

The P3DP samples were obtained in form of films via the electrochemical oxidation of the 3*n*-decylpyrrole dissolved in propylene carbonate with *p*-toluene sulphonate (tosylate) (Ts^-) as dopant electrolyte. The concentration of the dopant in the final product is about one counterion for each four to five pyrrole rings. The electrochemical deposition was carried out with a current density of 0.05 mA cm^{-2} under isothermal conditions at 298 K and in nitrogen atmosphere.

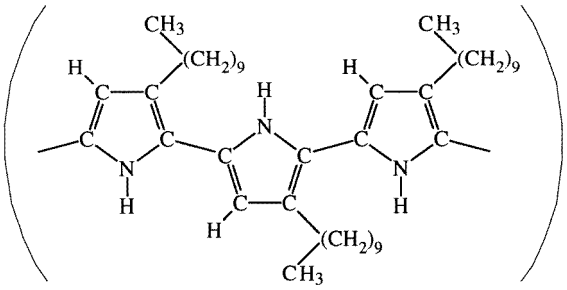

Poly(3n.-decylpyrrole) (P3DP)

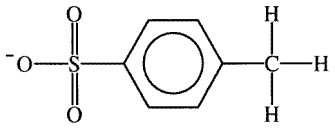

Tosylate anion (Ts^-)

Figure 2. The molecular structures of poly(3*n*-decylpyrrole) and tosylate counterion.

The d.c. conductivity of the samples measured at 298 K was $(2.7 \pm 0.3) \times 10^{-2}$ S m^{-1}. Such a value is four or five orders of magnitude lower than that of a polypyrrole doped at the same level [51, 52]. In fact, although the presence of alkylic chains increases the processability of the polymer, both the side chain and the size of counterions can hinder a regular and close-packed arrangement of the macromolecules [53].

3.2. Measurement methods

The d.c. conductivity of the sample films inserted in a four-gold-parallel-contact cell was measured in the temperature interval 80–330 K by a Schlumberger Solartron voltmeter 7081; the d.c. current was supplied by a Keithley generator 2202.

For the impedance measurements, disc shaped films inserted in a parallel golden plate capacitor were used. The admittance was measured for temperatures from 80 to 330 K and in the frequency range 100 Hz–40 MHz using an HP4194A impedance analyser. Measurements were carried out on samples of different thickness (90 and 120 μm). As the measured conductance and capacitance were inversely proportional to the sample thickness, the occurrence of spurious contact effects can be excluded. Also the I–V-characteristic of P3DP films was linear within about 0.2%, for applied electric fields lower than 10^3 V m^{-1}, so that no space charges developed at the electrode–sample interfaces. The d.c. conductivity, as measured by the parallel plate capacitor, was equal to that measured by the four-contact cell; this indicates that the interface effects were negligible. Moreover there was no significant anisotropy of the electrical conductivity of films. This behaviour was found also for polypyrrole doped by tosylate [54].

4. Results and discussion

4.1. D.c. behaviour

The d.c. conductivity data of P3DP films for temperatures from 330 to 90 K are shown in figure 3. The experimental data were suitably fitted by (1) taking into account a few hints by Hill [14]. The value of γ was obtained by the linear fit of the logarithm of activation energy, $\Delta E = -\mathrm{d}[\log_e(\sigma_{dc})]/\mathrm{d}[1/k_bT]$, versus $\log_e(1/k_BT)$ (see figure 4). The obtained value, $\gamma = 0.51 \pm 0.01$, is in good agreement with the values reported in the literature for a large number of amorphous semiconductors. Subsequently, the parameters A and T_0 were calculated by fitting the experimental data by (1) and assuming for b the theoretical value -1, which corresponds to $\gamma = 1/2$ (see previous section). The validity of the assumed b-value was also confirmed by comparing the residues of the fits with different values of b in the $[-1, 1]$ interval. The calculated parameters were: $b = -1$; $\gamma = 0.51 \pm 0.01$; $A = 26.6 \pm 0.2$ S m^{-1} K^{-1}; $T_0 = (4.7 \pm 0.1) \times 10^4$ K. The activation energy, ΔE, represents the maximum of the energy differences between couples of localized states allowing the hopping charge transport along a percolation path [27]. In the considered temperature interval, ΔE increases with temperature from 0.1 to 0.18 eV; these values agree with those for films of polypyrrole and its derivatives of comparable conductivity, measured elsewhere [10, 53, 55]. The observed temperature behaviour well matches the VRH model and moreover indicates that the transport mechanism is scarcely affected by the viscosity. This conclusion is also confirmed by experiments carried out in different conducting polymers, where a conductivity rise was observed by increasing the applied pressure [56–59]. In fact, if the viscosity were influent, the reduction of the free volume under pressure would lead to a decrease of the conductivity and to an increase of activation energy.

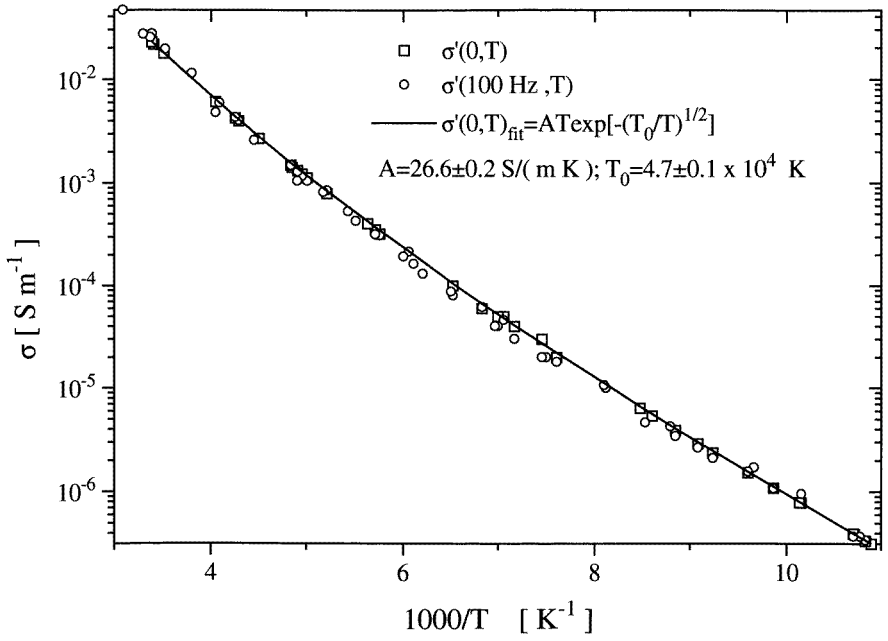

Figure 3. D.c. (square) and a.c. (circles) conductivity at 100 Hz in a log scale plotted against $1000/T$. Solid line from the fit equation.

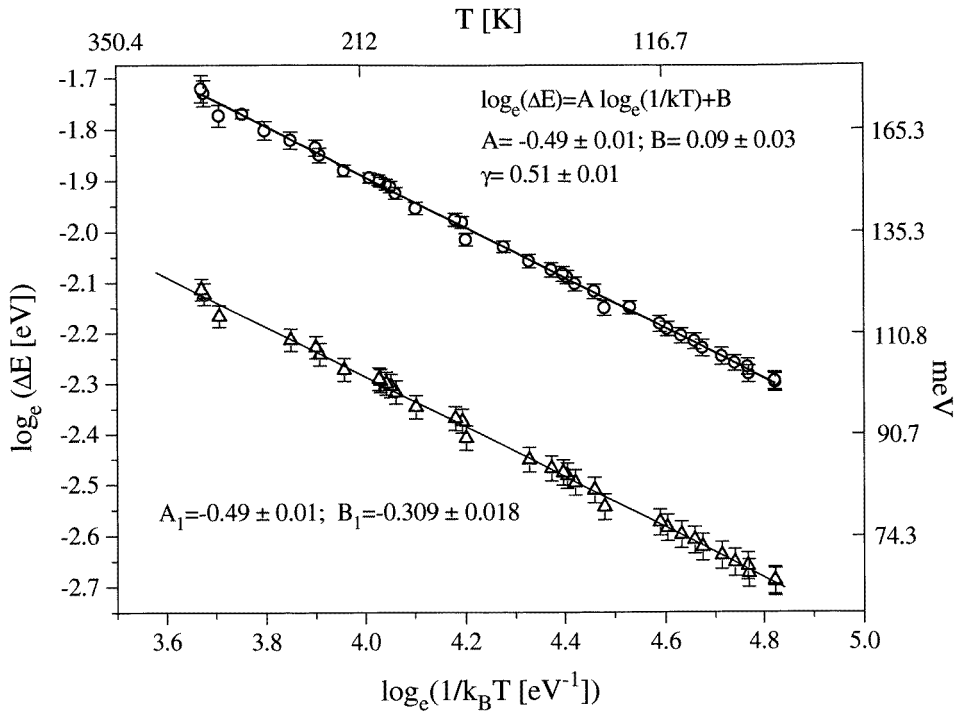

Figure 4. Plot of $\log_e(\Delta E)$ of the d.c. conductivity (circles) and angular frequency of the loss peak (triangles) against $\log_e(1/k_BT)$. Solid lines represent the apparent linear fits.

4.2. A.c. behaviour

The real part of the permittivity, $\varepsilon'(\omega)$, and the real a.c. conductivity, $\sigma'(\omega)$, at different temperatures, as determined by the admittance measurements, are plotted in figures 5(a) and (b), respectively. $\sigma'(\omega)$ maintains a stable value ($\sigma'(\omega) = \sigma_{dc}$) up to a frequency where it begins to monotonically increase (figure 5(a)). The frequency at which the slope of the conductivity changes increases with temperature, and, for frequencies where $\sigma'(\omega) \gg \sigma_{dc}$, $\sigma'(\omega)$ approaches a power law behaviour. The temperature dependence of the a.c. conductivity at low frequency is the same as that of the d.c. conductivity; that is shown in figure 3 for 100 Hz. The coincidence of the temperature dependences of σ_{dc} and $\sigma'(\omega)$ at low frequencies confirms that the electrode polarization effects are negligible. For higher frequencies, $\sigma'(\omega)$ displays a weaker temperature dependence (figure 5(a)). The measured values of ε' are rather large and greatly increase with temperature (figure 5(b)). The anomalous rise of ε' in the low frequency side of the spectrum resembles that observed in many other systems, and can be related to the low frequency dispersion (LFD) [60, 61]. This effect becomes evident below a characteristic frequency, which decreases as the temperature decreases [62]. This assignment is also supported by the observation that, at low frequency, the logarithmic slope of ε' against frequency is slightly greater than -1, and the ε' values are not very sensitive to the change of the electric field amplitude. In fact, if there were any Maxwell–Wagner or electrode polarization phenomenon, a stronger dependence of ε' would be observed on both the electric field amplitude and frequency; also the slope in the log scale against frequency should fall between -2 and -1 [61, 63–65].

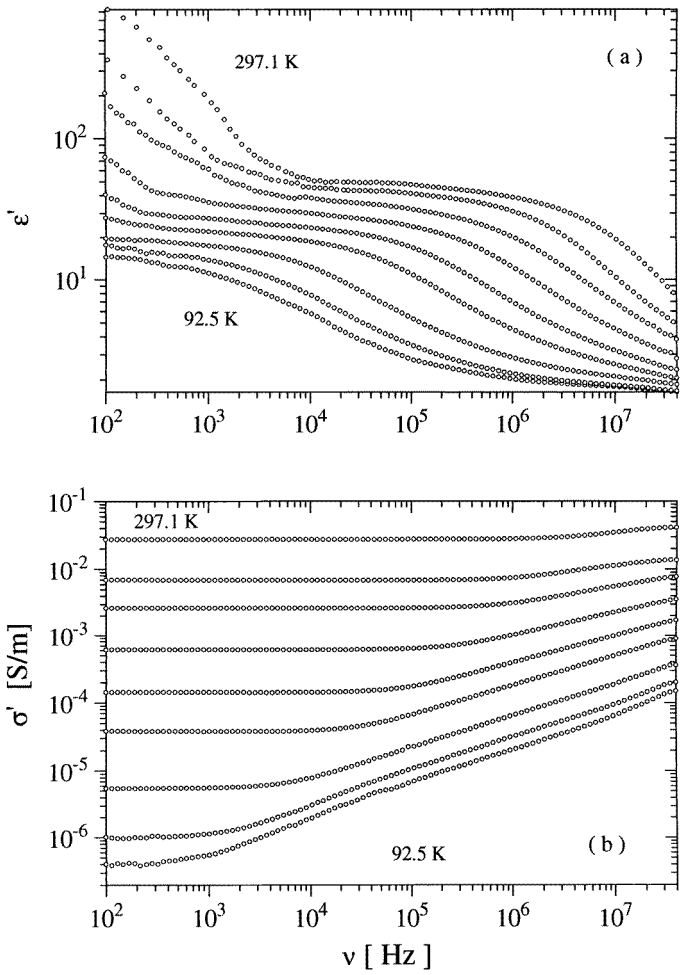

Figure 5. (a) Log–log plot of the real part ε' of the permittivity against frequency ν at selected temperatures $T = 297.1$ K, 247.4 K, 219.0 K, 185.7 K, 157.6 K, 138.7 K, 115.8 K, 99.6 K, 92.5 K in the order from upper to lower spectra. (b) Log–log plot of the real part σ' of the conductivity against frequency ν at selected temperatures $T = 297.1$ K, 247.4 K, 219.0 K, 185.7 K, 157.6 K, 138.7 K, 115.8 K, 99.6 K, 92.5 K in the order from upper to lower spectra.

At higher frequencies, a dielectric-like relaxation can be recognized. In fact, the observed decrease of ε' parallels an evident change of the slope of $\sigma'(\omega)$ (figures 5(a) and (b)), and both these effects shift towards low frequencies as the temperature decreases. This is confirmed by the plot of the quantity $\varepsilon''_d(\omega)$ (3) as a function of frequency (figure 6) which shows a loss peak together with a decrease of $\varepsilon'(\omega)$. At low frequency, $\sigma'(\omega) \sim \sigma_{dc}$ and $\varepsilon''(\omega)$ reaches $\sigma_{dc}/(\varepsilon_0\omega)$ so that the values of $\varepsilon''_d(\omega)$ become less accurate; these data have been omitted from figure 6.

At this point we should decide whether the observed relaxation is related either to the hopping charge conductivity or rather to the bound charge motions. In a system where the hopping charge transport is the unique phenomenon affecting the electric response, (14) provides the frequency value at which the conductivity begins to depend on frequency. The order of magnitude of such a frequency value can be appraised by considering the frequency

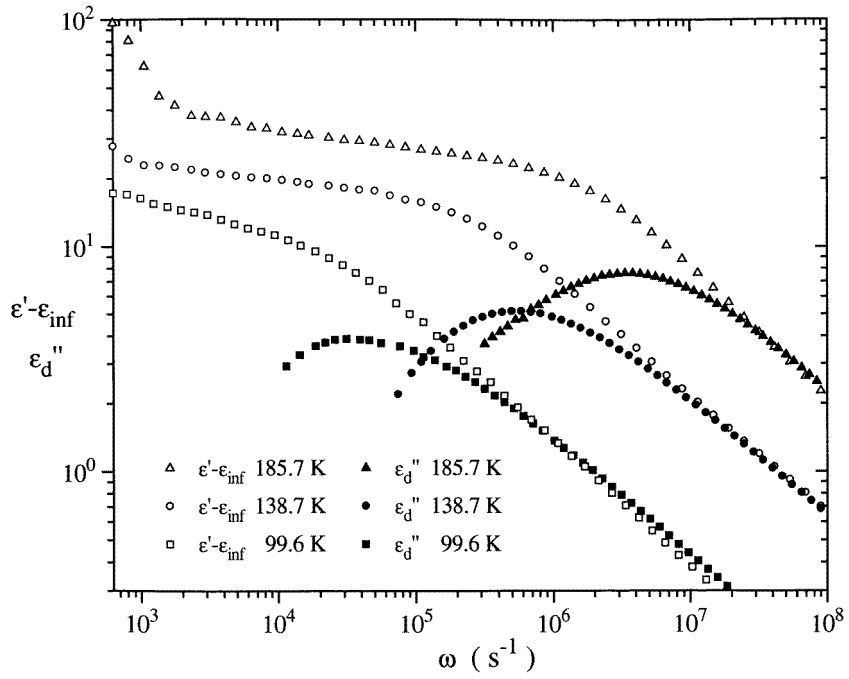

Figure 6. The quantity $[\varepsilon(\nu) - \varepsilon_\infty]$ and ε_d'' for different temperatures plotted against the angular frequency ω in a log–log scale.

$\omega_s = \sigma_{dc}/(\Delta\varepsilon\,\varepsilon_0)$, corresponding to the assumption $p = 1$. In this case, the loss peak can be only found in the plot of the quantity $\varepsilon_d''(\omega) = \varepsilon''(\omega) - \sigma_{dc}/(\varepsilon_0\omega)$, and it is never observable in the plot of the dielectric loss $\varepsilon''(\omega)$. This behaviour is a consequence of the fact that the d.c. and a.c. responses are produced by the same transport phenomenon, and the system behaviour fulfils the BNN condition [27]. However, such an electric response cannot be considered as peculiar to the hopping charge transport; in fact, it could be also observed in the presence of a dipolar relaxation superimposed on a frequency independent conductivity. To explain better, let us consider an ideal system where the normalized dielectric response, $\varepsilon_n^*(\omega, T)$, is a superposition of a dipolar relaxation, which for simplicity we suppose Debye-like, and a frequency-independent conductivity:

$$\varepsilon_n^*(\omega, T) = \frac{\varepsilon^*(\omega) - \varepsilon_\infty}{\Delta\varepsilon} = \frac{1}{1 + \mathrm{i}\omega\tau} - \mathrm{i}\frac{\sigma_{dc}}{\varepsilon_0\omega\,\Delta\varepsilon}. \tag{16}$$

By defining $\omega_s = 1/\tau_s = \sigma_{dc}/(\varepsilon_0\,\Delta\varepsilon)$, $\varepsilon_n^*(\omega, T)$ becomes:

$$\varepsilon_n^*\left(\frac{\omega}{\omega_s}, T\right) = \frac{1}{1 + \mathrm{i}(\omega/\omega_s)\tau/\tau_s} - \mathrm{i}\frac{\omega_s}{\omega} \tag{17}$$

i.e., it becomes dependent on the term τ/τ_s when plotted against ω/ω_s. The real and the imaginary parts of (17) have been plotted in figure 7 for three different values of the ratio τ/τ_s. It is apparent that, as τ/τ_s decreases, the imaginary part of ε_n^* shows a relaxation peak only when τ/τ_s becomes less than 1; in other words, when $\tau/\tau_s \geqslant 1$ the relaxation peak of $\varepsilon''(\omega)$ practically disappears, and the response is dominated by the d.c. behaviour. As in a polar dielectric system the ratio τ/τ_s depends on temperature, then suitable values of τ/τ_s, i.e., less than 1, to put in evidence the peak relaxation in the imaginary part of

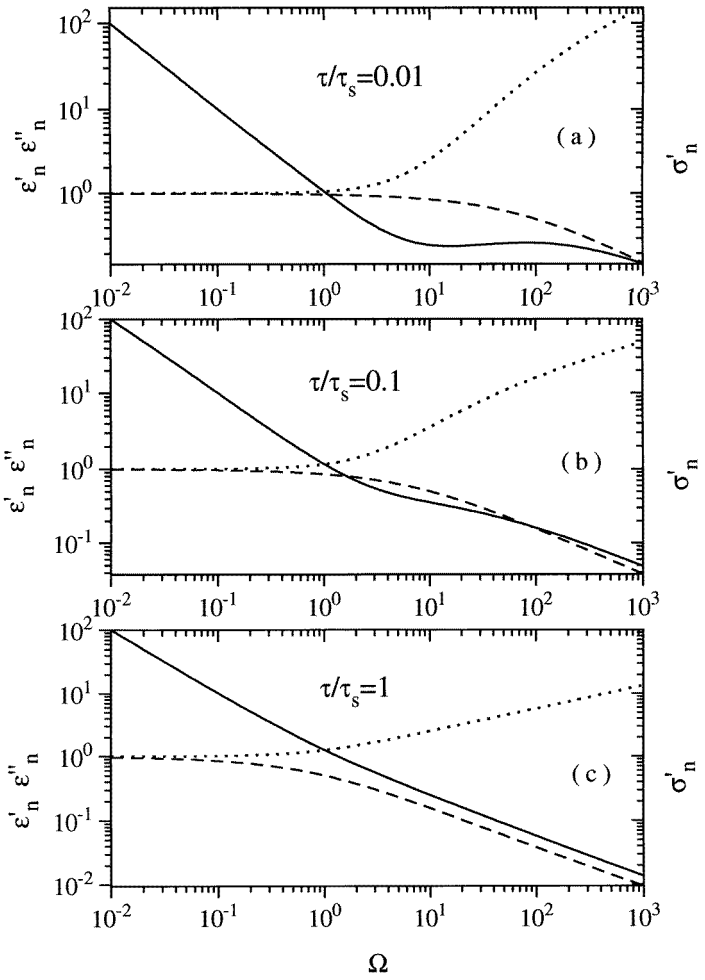

Figure 7. The real, ε_n' (solid line), and imaginary, ε_n'' (dashed line), parts of the normalized dielectric response plotted against $\Omega = \omega/\omega_s$ in a log–log scale for different values of the ratio τ/τ_s. On the same scale, the real part of the normalized conductivity, σ_n' (dotted line), is shown.

ε_n, can be eventually reached by changing the temperature. However, in many systems, where conductivity and dipolar relaxation are coupled each other by viscosity, the product $\sigma(T)\tau(T)$ is independent of temperature and the quantity:

$$p = \frac{\tau}{\tau_s} = \frac{\tau(T)\sigma(T)}{\Delta\varepsilon(T)\varepsilon_0} \tag{18}$$

can become a quasi-constant and close to 1, so that the relaxation peak of $\varepsilon''(\omega)$ can no longer be observed. As (18) coincides with the BNN condition, it is impossible to distinguish, without additional information, if the electric response originates from dipoles rather than from hopping charges.

Significant information to check the nature of the electric response can be obtained by analysing the temperature behaviour of the conductivity, relaxation strength and frequency of the loss peak, as carried out by other authors. These parameters can be extracted by fitting the permittivity spectra with the following equation:

$$\varepsilon(\omega) = \varepsilon_\infty + (\varepsilon_s - \varepsilon_\infty)H(\omega) - \mathrm{i}\frac{\sigma_{dc}}{\varepsilon_0\omega} + \frac{B}{\varepsilon_0}(\mathrm{i}\omega)^{(n-1)} \tag{19}$$

where $H(\omega) = [1 + (\mathrm{i}\omega\tau)^{(1-\alpha)}]^{-\beta}$ represents the normalized Havriliak–Negami relaxation function (HN); $(\mathrm{i}\sigma_{dc}/\varepsilon_0\omega)$ is the d.c. conductivity contribution, and $B(\mathrm{i}\omega)^{n-1}/\varepsilon_0$ describes the effect of the low frequency dispersion (LFD); B is a constant and $n < 1$ [62]. Equation (19) accounts for the presence of a relaxation phenomenon, whatever the origin, and for a charge transport contribution in phase with the driving electric field. The fit of the experimental data by (19) was carried out using a complex non-linear least square procedure which simultaneously minimizes the deviations of both the real and imaginary parts, by taking into account the Kramers–Kronig relations [65]. The fit obtained by (19) is plotted in figure 8 where each of the three different contributions is also indicated. The

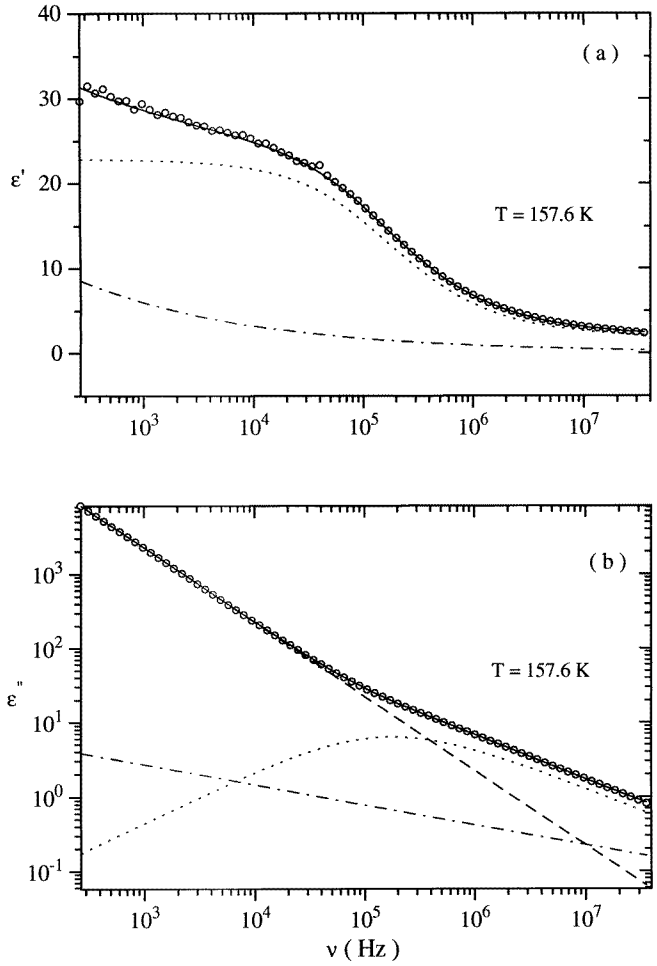

Figure 8. (a) The real part, ε', of the permittivity at 157.6 K plotted against log of frequency ν. The resulting fit (solid line) sums up the HN (short dashed line) and LFD (dashed–dotted line) contributions. (b) The imaginary part, ε'', of the permittivity at 157.6 K plotted against log of frequency ν. The resulting fit (solid line) sums up the HN (short dashed line), LFD (dashed–dotted line) and the d.c., $\sigma_{dc}/\omega\varepsilon_0$ (dashed line) contributions.

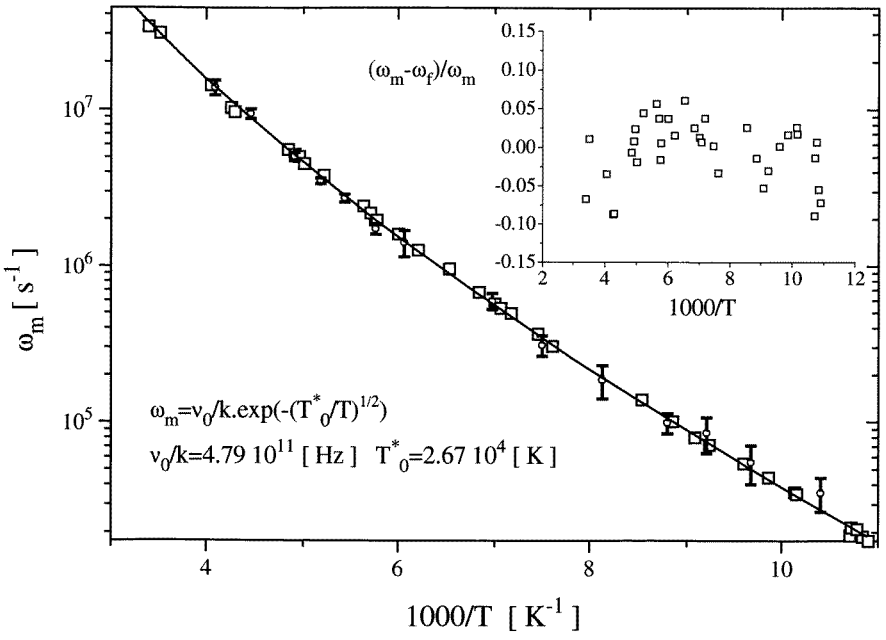

Figure 9. The Arrhenius plot of the angular frequency ω_m against the reciprocal temperature $1000/T$. The squares are the frequencies of the loss peak calculated by the fit; the circles represent the frequencies of the loss peak directly determined from the spectra of $\varepsilon''(\omega)$. The solid line is (13). In the inset, the residues against reciprocal temperature are shown.

LFD contribution to $\varepsilon'(\omega)$ is appreciable in the frequency interval where $\varepsilon'(\omega)$ should be constant, while the contribution to $\varepsilon''(\omega)$ is negligible in the same frequency range as the d.c. conduction effect is dominant. Though the chi-square value is quite reasonable, the residues show that the experimental data on the high frequency tails are not well fitted by (19). The frequency ω_m of the loss peak was either directly determined from the spectra or calculated by the relaxation time provided by the fitting. The quantity ω_m was plotted in an Arrhenius plot against reciprocal temperature in order to show that the activation energy is slightly increasing with temperature (figure 9). The behaviour of ω_m parallels that of the d.c. conductivity; in fact $\log_{10}(\omega_m)$ matches a power law behaviour versus reciprocal temperature with an exponent $1/2$ (solid line in figure 9). That is the opposite of that occurring in a dielectric relaxation process, where due to cooperative phenomena the activation energy decreases as the temperature rises [66]. It is obvious that this behaviour cannot be attributed to a main dipolar relaxation process. Also the rise of the relaxation strength with temperature would be very unusual for a dipolar relaxation (figure 10). Moreover, as the value of the ε' plateau is rather large (around 60 at room temperature), it is not likely to arise from molecular dipoles, also considering that the apparent density of the material is quite low (0.5 g cm^{-3}). Such a large value of the polarization could rather be provided by delocalized charges on the oxidized macromolecule and by tosylate counterions bound to the molecular chain defects. This conclusion definitely relates the dielectric response to those charge carriers which cause the d.c. conductivity. On the other hand, the contribution to the observed relaxation of weakly bound charge carriers was observed in many other materials, as well as ionic and electronic glasses, amorphous semiconductors, transition-metal oxides and sulphides [21, 43, 45, 67–69], metal-cluster compounds, cermets and carbon-polymer composites [61],

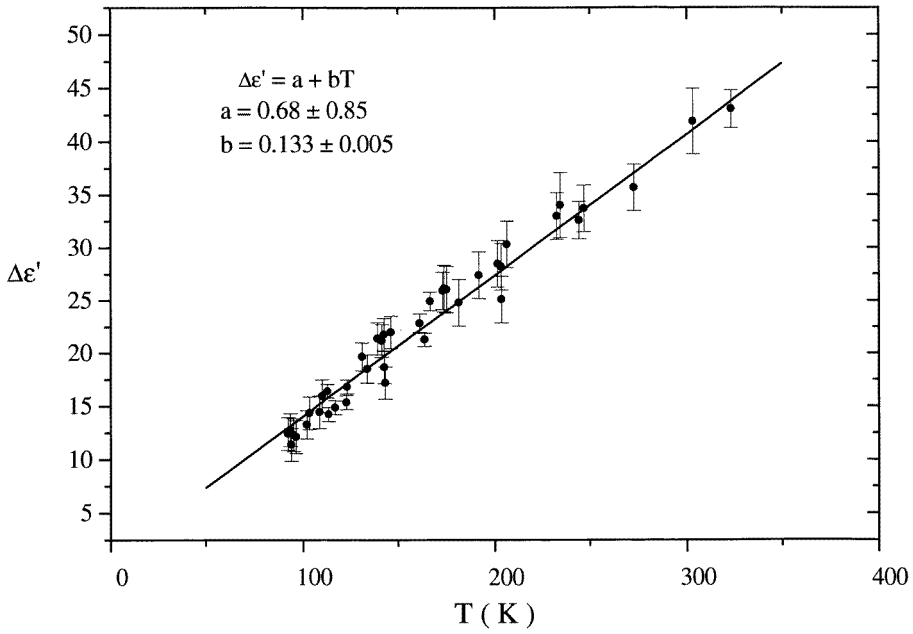

Figure 10. The relaxation strength plotted against temperature T. Solid line from fit equation.

where the hopping conduction mechanism is clearly recognized. In such materials the contribution of the dipolar orientation is weak and the electric response is dominated by diffusive charge hopping processes, involving both ionic and electronic carriers. All materials, where the conductivity arises from diffusive hopping or tunnelling of charge carriers among randomly distribute sites, show very striking similarities [26, 27]. Similar properties have been also observed in the dielectric response of different polymeric materials, as well as polyaniline [70–73], polypyrrole [74–79] and other conducting polymers [80–82] having conductivity values close to those of the semiconductors. Recent experiments on polypyrrole stated a strong correlation between dielectric response and d.c. conductivity, as this latter and the frequency of the loss peak meet the BNN condition [78, 79, 83]. On this basis, we gained the conviction that even the overall electric response of the poorly conducting polymer here considered could conveniently be analysed within the frame of theories developed for describing the charge transport mechanism in disordered systems.

Despite the high doping level, the polymer here considered exhibits a low value ($\sigma_{298} = 2.7 \times 10^{-2}$ S m^{-1} at 298 K) and a considerable variation of d.c. conductivity with temperature ($\log_{10}(\sigma_{298}/\sigma_{90}) \approx 5$), due to large interchain separation and disorder, which make difficult the charge transport through the material. In this condition the system is well away from the insulator–metal transition [16, 18], and therefore the hopping models should well describe the electrical response in the whole temperature and frequency range.

To relate the electric response to a hopping charge transport, three main requirements have to be satisfied:

(i) the d.c. conductivity must originate from hopping charge transport;

(ii) the relaxation strength must depend on temperature as the preexponential factor $\sigma_0(T)$ of the d.c. conductivity;

(iii) the frequency of the loss peak observed in $\varepsilon_d''(\omega)$ must depend on temperature with the same exponential law as the d.c. conductivity.

The requirements (i) and (ii) are equivalent to the BNN condition between ω_m and σ_{dc}. As previously discussed, the system here analysed well fulfils the requirement (i). The temperature dependence of the relaxation strength $\Delta\varepsilon$ is almost linear (figure 10), just as for the prefactor $\sigma_0(T)$ (see (12)), and then it fulfils the requirement (ii). Though this behaviour seems to be unusual, also other materials, such as metal cluster compounds [61] whose d.c. conductivity behaviour is describable by the Mott law (1) with $\gamma = 1/2$, show a relaxation strength increasing with temperature. In contrast, in those systems where the conductivity scales with the exponent $\gamma = 1/4$, the relaxation strength decreases with increasing temperature [55, 78, 79]. This result agrees with theoretical predictions previously quoted, which state that in (1), for $\gamma = 1/2$, b is -1, and, for $\gamma = 1/4$, b is $1/2$. Finally, the temperature behaviour of the frequency peak ω_m is well fitted by (13) for $\gamma = 1/2$ (figure 9); the calculated fit parameters are:

$$\nu_0/k = 4.79 \times 10^{11} \text{ Hz} \qquad T_0^* = 2.67 \times 10^4 \text{ K}.$$

As expected [37] the factor ν_0/k is of the order of the phonon frequency. The residues drawn in the inset of figure 9 are randomly distributed around zero and demonstrate the very good agreement between the experimental data and the theoretical prediction provided by (13). However, the temperature parameter T_0^* for ω_m is smaller by a factor 1.76 than the corresponding parameter T_0 for the conductivity; this means that the activation energy of the relaxation ($\Delta E = 0.12$ eV at 300 K) is smaller than that of the d.c. conductivity ($\Delta E = 0.18$ eV at 300 K). As shown in figure 4, the activation energy, as well as the d.c. conductivity, increases with temperature, thus confirming the common origin of the charge transport mechanism and the relaxation. In fact, such a temperature behaviour cannot occur in the presence of a viscous coupling between these two phenomena, which conversely could lead to fulfilment of the BNN condition.

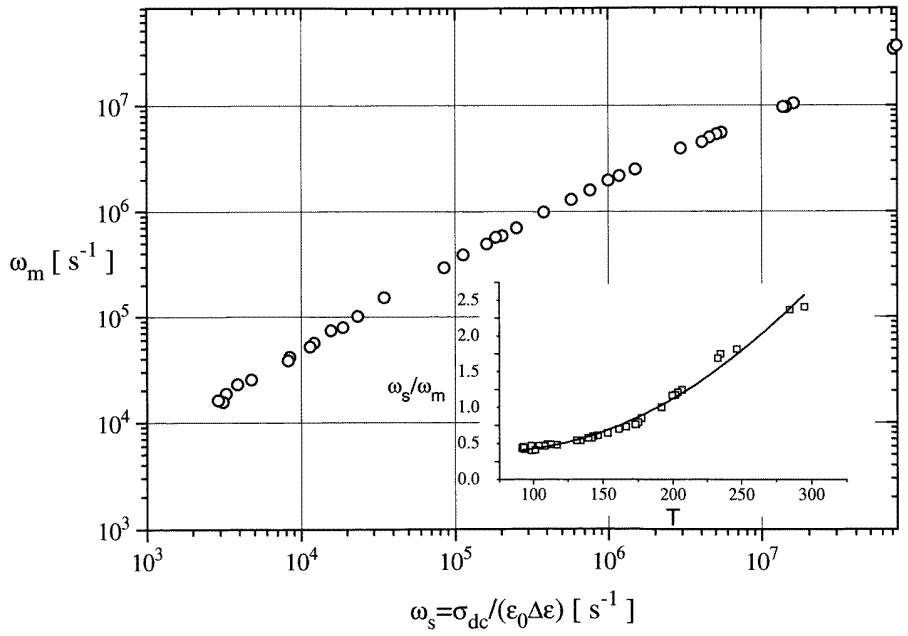

Figure 11. The angular frequency, ω_m, of the loss peak plotted against the angular frequency, $\omega_s = \sigma_{dc}/\varepsilon_0\,\Delta\varepsilon$. In the inset the ratio ω_s/ω_m is plotted against temperature T.

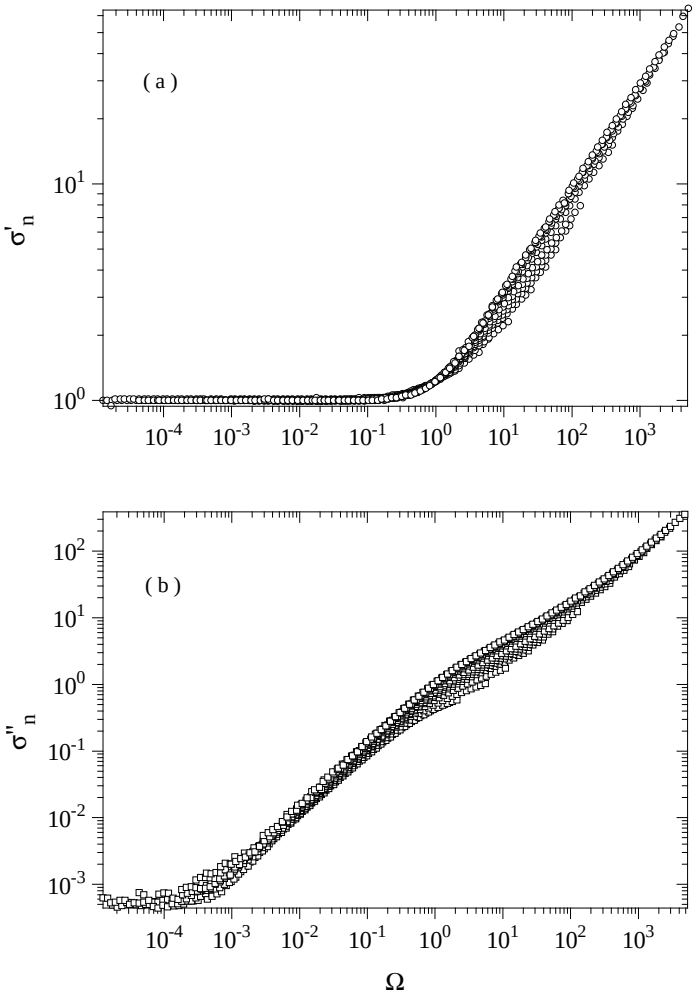

Figure 12. (a) Plot of the real part, σ_n', of the normalized conductivity against $\Omega = \omega/\omega_s$. The data relate to the temperature interval 100–295 K. (b) Plot of the imaginary part, σ_n'', of the normalized conductivity against $\Omega = \omega/\omega_s$ calculated by using the same data as (a). The data relate to the temperature interval 100–295 K.

The intermediate frequency hopping theories do not predict an activation energy for the relaxation loss less than that of the d.c. conductivity; however, this fact is reasonably expected by taking into account that the d.c. conductivity is essentially determined by the jumps having the highest energy barriers, while the a.c. conductivity at the frequency $\omega_m \cong \omega_s$ is determined by the charge carriers diffusing on short distances, i.e., by the jumps having the lowest energy barriers [78]. At high frequency, especially at low temperatures, the contribution to the electrical response due to carriers hopping among few neighbour sites is not negligible. In this regime, where the pair approximation [25] becomes valid, the a.c. electric response is no longer closely related to the d.c. conductivity [43]. Some discrepancies concerning the predictions of intermediate frequency hopping theories can arise from an additional contribution of charges hopping between two sites only.

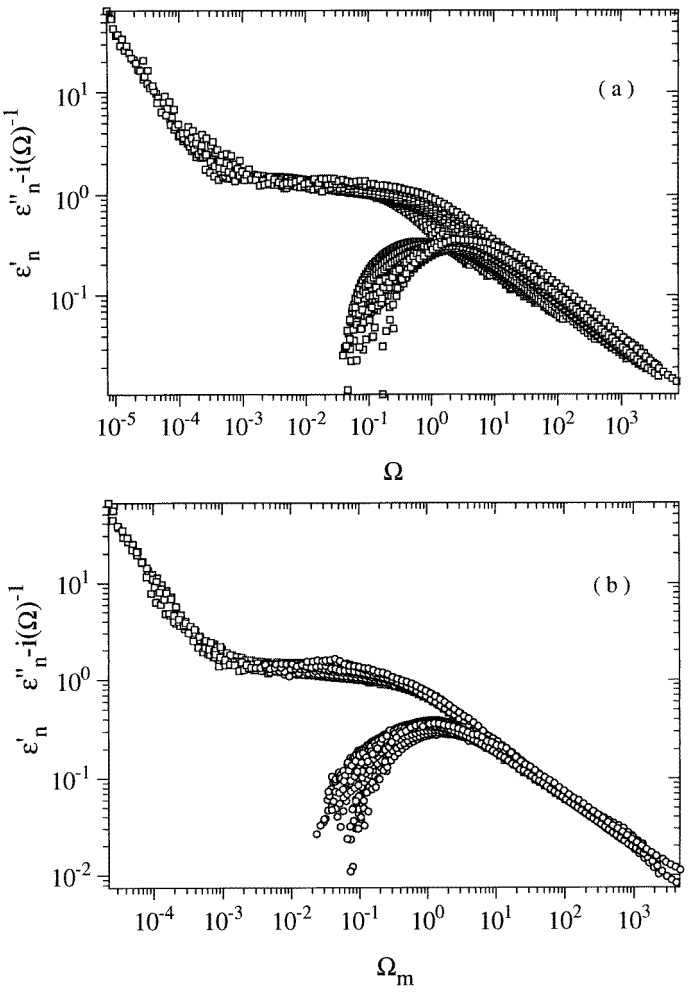

Figure 13. (a) The real, ε'_n, and imaginary, $\varepsilon''_n - \mathrm{i}(\Omega)^{-1}$, parts of the normalized permittivity are plotted against $\Omega = \omega/\omega_s$ in the temperature interval 100–295 K. (b) The real, ε'_n, and imaginary, $\varepsilon''_n - \mathrm{i}(\Omega)^{-1}$, parts of the normalized permittivity are plotted against $\Omega_m = \omega/\omega_m$. The data are the same as in (a).

According to (14), if the frequency ω_m of the loss peak for each temperature is proportional to the quantity $\omega_s(T) = \sigma_{dc}(T)/(\varepsilon_0\,\Delta\varepsilon(T))$, the BNN relation is fulfilled. The data drawn in figure 11 roughly meet the BNN relation, while the ratio ω_s/ω_m varies from 0.5 to 2.5, as shown in the inset. This result corresponds to a lack of selfsimilarity of the normalized complex conductivity, σ_n^*, as a function of the dimensionless frequency $\Omega = \omega/\omega_s$ (figure 12). Though a complete superposition of the normalized conductivity (different curves in figure 12) is not verified, it has to be taken into account that the conduction phenomena are also accompanied by dielectric effects. The selfsimilarity can be tested also for $(\varepsilon' - \varepsilon_\infty)/\Delta\varepsilon$ and $\varepsilon''_d/\Delta\varepsilon$ versus the same variable Ω (figure 13(a)), leading to the same conclusion. However, if the previous quantities are plotted versus $\Omega_m = \omega/\omega_m = p(T)\omega/\omega_s$ (i.e., scaled against the frequency of the loss peak) a more satisfactory selfsimilar behaviour is obtained (figure 13(b)). On these bases, we conclude

that the behaviour of the complex permittivity is essentially independent of temperature (i.e., selfsimilar); however the scaling variable is different from that predicted by BNN. The last remark concerns the low frequency tail of the relaxation peak, which shows a log slope value smaller than that (about 2) predicted by the intermediate frequency hopping models; however, this behaviour was previously observed also in other materials [27, 36].

A deeper qualitative comparison between a description based on hopping theories and on the Havriliak–Negami function can be performed by analysing the coefficients s' and s'' defined by (15*a*) and (15*b*), and plotted in figure 1(b). There are two main differences between the behaviour predicted by EMA (figure 1(b)) and that represented by the HN dielectric function, i.e., the existence of the crossing point between s' and s'' and a slightly increase of both parameters, which never coincide, as the frequency increases up to the highest values. In other terms, while the behaviours of s-parameters are almost similar in the low frequency region, just above the critical frequency the behaviour predicted by the EMA model diverges from the power law trend of the HN function.

The experimental data and theoretical predictions can be compared by plotting s' and s'' versus the normalized frequency $\Omega = \omega/\omega_s$ (figure 14). The data related to different temperatures almost overlap, so that a common behaviour as predicted by intermediate frequency hopping models can be recognized. In particular, the low frequency trend for $s' \approx 2$ and $s'' \approx 1$ and the existence of a crossing point at high frequency well match the theoretical predictions. The two s-parameters do not tend asymptotically to the same high frequency value, as should occur if the HN function were a valid representation; on the contrary, above a given frequency Ω, s'' becomes greater than s', according to the prediction of the intermediate frequency hopping models. For higher Ω, many theories

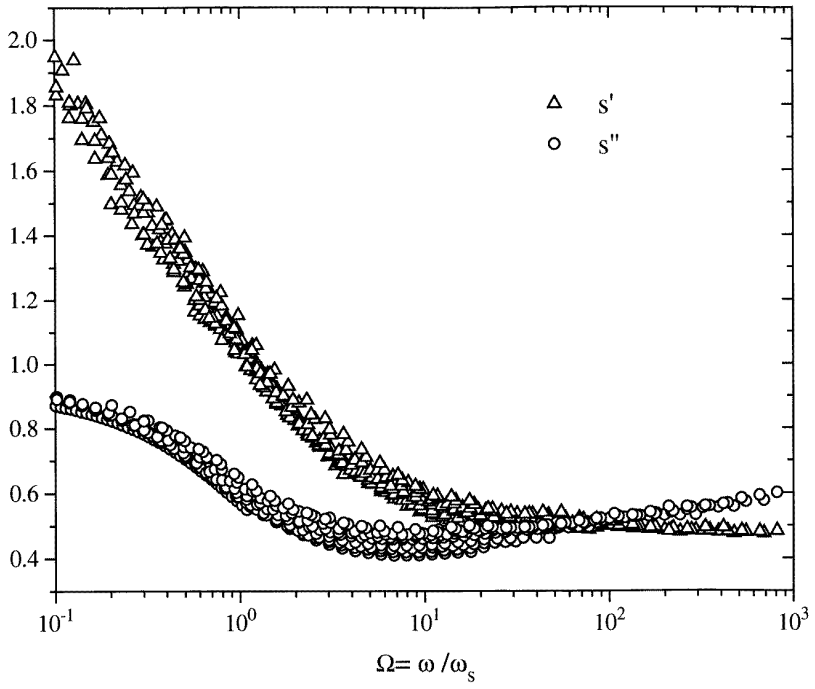

Figure 14. Plot of s' and s'' against $\Omega = \omega/\omega_s$ calculated from the spectra in the temperature interval 100–295 K.

predict a transition to the pair approximation (PA) regime. PA models typically predict $\sigma''/\sigma' \propto \ln(\nu_0/\omega)$ [25, 43, 44], which means $s'' < s'$. But $s' < s''$ at high Ω and $s'' - s'$ does not decrease (figure 14); accordingly the transition to the PA regime, if it occurs, should be at higher Ω.

Some words are necessary to comment on the presence of a low frequency dispersion (LFD) effect. It is generally accepted that LFD cannot be explained by the intermediate frequency hopping models [62], and this fact leads to the conclusion that the two phenomena have different origin. However, we observed that the scaling behaviour of LFD parallels that of the loss peak (figure 13(b)). This result was also found by van Staveren for some metal cluster compounds where the conduction is undoubtedly caused by the hopping charge transport [61]. Then, in our opinion, it is difficult to consider the two phenomena as not related each other.

5. Conclusions

The d.c. conductivity and the electric a.c. response up to 40 MHz of poly(3*n*-decylpyrrole), as measured from 80 up to 330 K, provided valuable information to characterize the charge transport behaviour of the system. The d.c. conductivity well fits the VRH model. As the conductivity starts to depend on frequency, a loss peak was observed. The frequency of this loss peak shows a temperature dependence which coincides with that observed for d.c. conductivity; the strength of this relaxation increases with temperature and becomes too large to be related to a dipolar relaxation. On the other hand, the theoretical models for the hopping charge transport predict the existence of a loss peak like that observed. The most obvious conclusion is that a unique charge hopping process produces both the observed d.c. and a.c. conductivities; this accounts also for the observed temperature behaviour of the activation energy and frequency of the loss peak. The increase of the conductivity activation energy with temperature and of the conductivity with the pressure can be explained by the increase of the localized state density near the Fermi level. No viscosity effects can be envisaged, as, in those systems where the conductivity is strongly related to the viscosity, the conductivity activation energy decreases with temperature and increases with pressure. Moreover, as the dipolar relaxation is also dominated by viscosity, the temperature behaviour of the loss peak is a good test to decide what is the origin of the observed relaxation.

A further confirmation that the observed relaxation has its origin in the hopping charge transport is given by the temperature behaviour of the relaxation strength and the frequency dependence of s'- and s'' coefficients.

In contrast, the theoretical prediction concerning the selfsimilarity of the a.c. conductivity is roughly verified, as the activation energy of σ_{dc} is slightly different from that of ω_m; also the overall behaviours of the conductivity and permittivity are not well fitted by the theoretical models which lead to a selfsimilar behaviour. Several causes can be envisaged to explain these discrepancies:

(i) the proposed models are based on very general assumptions which do not take into account the material characteristics and the nature of charge carriers;

(ii) all the models consider the fixed hopping mechanism only; the VRH is considered by introducing some corrective terms only;

(iii) the hopping transport mechanism is generally accompanied by other effects, such as dipolar relaxation and many body long range interactions, which are not taken into account and

(iv) the lack of selfsimilar behaviour could be related to the contribution of charges hopping between only two sites.

References

[1] Ruggeri G, Bianchi M, Puccioni G and Ciardelli F 1997 *Pure Appl. Chem.* **69** 143
[2] Skotheim T A 1986 *Handbook of Conducting Polymer* vols 1, 2 (New York: Dekker)
[3] Bredas J L (ed) 1991 *Conjugated Polymers: the Novel Science and Technology of Highly Conducting and Nonlinear Optically Active Materials* (Dordrecht: Kluwer)
[4] Yu S and Lu J 1988 *Solitons and Polarons in Conducting Polymers* (Singapore: World Scientific)
[5] Su W P, Schrieffer J R and Heeger A J 1979 *Phys. Rev. Lett.* **42** 1698
[6] Heeger A J, Kivelson S, Schrieffer J R and Su W P 1988 *Rev. Mod. Phys.* **60** 781
[7] Scott J C, Pfluger P, Krounbi M T and Street G B 1983 *Phys. Rev.* B **28** 2140
[8] Kivelson S 1982 *Phys. Rev.* B **25** 3798
[9] Bredas J L, Chance R R and Silbey R 1982 *Phys. Rev.* B **26** 5843
[10] Maddison D S and Tansley T L 1992 *J. Appl. Phys.* **72** 4677
[11] Roth S 1991 *Hopping Transport in Solids* ed M Pollak and B I Shklovskii (Amsterdam: North-Holland) pp 377–95
[12] Ezquerra T A, Rühe J and Wegner G 1988 *Chem. Phys. Lett.* **144** 194
[13] Zuppiroli L, Bussac M N, Paschen S, Chauvet O and Forro L 1994 *Phys. Rev.* B **50** 5196
[14] Hill R M 1976 *Phys. Status Solidi* a **35** K29
[15] Sheng P and Klafter J 1983 *Phys. Rev.* B **27** 2583
[16] Epstein A J, Joo J, Kohlman R S, Du G, MacDiarmid A G, Oh E G, Min Y, Tsukamoto J, Kaneko H and Pouget J P 1994 *Synth. Met.* **65** 149
[17] Yoon C O, Reghu M, Moses D, Heeger A J, Cao Y, Chen T-A, Wu X and Rieke R D 1995 *Synth. Met.* **75** 229
[18] Kohlman R S, Joo J, Min Y G, MacDiarmid A G and Epstein A J 1996 *Phys. Rev. Lett.* **77** 2766
[19] Böttcher C J F and Bordewijk P 1978 *Theory of Electric Polarization* vol 2 (Amsterdam: Elsevier) p 18
[20] Böttger H and Bryksin V V 1985 *Hopping Conduction in Solids* (VCH: Weinheim)
[21] Mott N F and Davis E A 1979 *Electronic Processes in Noncrystalline Materials* (London: Oxford University Press)
[22] Efros A L and Shklovskii B I 1975 *J. Phys. C: Solid State Phys.* **8** L49
[23] Shklovskii B I and Efros A L 1984 *Electronic Properties of Doped Semiconductors* (Berlin: Springer)
[24] Ambegaokar V, Halperin B I and Langer J S 1971 *Phys. Rev.* B **4** 2612
[25] Seager C H and Pike G E 1974 *Phys. Rev.* B **10** 1435
[26] Hunt A 1991 *J. Phys.: Condens. Matter* **3** 7831
[27] Dyre J 1988 *J. Appl. Phys.* **64** 2456
[28] Pollak M and Geballe T H 1961 *Phys. Rev.* **122** 1742
[29] Bryksin V V 1980 *Sov. Phys.–Solid State* **22** 1421
[30] Summerfield S and Butcher P N 1982 *J. Phys. C: Solid State Phys.* **15** 7003
[31] Summerfield S and Butcher P N 1983 *J. Phys. C: Solid State Phys.* **16** 295
[32] Summerfield S 1985 *Phil. Mag.* B **52** 9
[33] Odagaki R and Lax M 1981 *Phys. Rev.* B **24** 5284
[34] Scher M and Lax M 1973 *Phys. Rev.* B **7** 4491
[35] Dyre J 1993 *Phys. Rev.* B **48** 12 511
[36] Long A R 1991 *Hopping Transport in Solids* ed M Pollak and B I Shklovskii (Amsterdam: North-Holland) pp 207–31
[37] Hunt A 1991 *Solid State Commun.* **80** 151
[38] Odagaki R and Lax M 1982 *Phys. Rev.* B **26** 6480
[39] Barton J L 1966 *Verres Réfr.* **20** 328
[40] Nakajima T 1971 *Ann. Rep. Conf. on Electric Insulation and Dielectric Phenomena* (Washington, DC: National Academy of Science) p 168
[41] Namikawa H 1975 *J. Non-Cryst. Solids* **18** 173
[42] Havriliak S, Jr and Negami S 1966 *J. Polym. Sci.* C **14** 99
[43] Long A R 1982 *Adv. Phys.* **31** 553
[44] Elliott S R 1987 *Adv. Phys.* **36** 135
[45] Mansingh A, Reyes J M and Sayer M 1972 *J. Non-Cryst. Solids* **7** 12

[46] Long A R, McMillan J, Balkan N and Summerfield S 1988 *Phil. Mag.* B **58** 153
[47] D'Arrigo P 1992 *Thesis* University of Pisa
[48] Bätz P, Schmeisser D and Göpel W 1991 *Phys. Rev.* B **43** 9178
[49] Schmeisser D and Göpel W 1993 *Ber. Bunsenges. Phys. Chem.* **97** 372
[50] Petrillo C, Borra S, Cagnolati R and Ruggeri G 1994 *J. Chem. Phys.* **101** 11 004
[51] Maddison D S, Unsworth J and Roberts R B 1988 *Synth. Met.* **26** 99
[52] Zuppiroli L, Paschen S and Bussac M N 1995 *Synth. Met.* **69** 621
[53] Wegner G and Rühe J 1989 *Faraday Discuss. Chem. Soc.* **88** 363
[54] Kiani M S and Mitchell G R 1993 *J. Phys. D: Appl. Phys.* **26** 1718
[55] Singh R, Narula A K, Tandon R P, Mansingh A and Chandra S 1996 *J. Appl. Phys.* **79** 1476
[56] Lundin A, Lundberg B, Sauerer W, Nandery P and Naegek D 1990 *Synth. Met.* **236**
[57] Maddison D S and Tansley T L 1992 *J. Appl. Phys.* **71** 1831
[58] Isotalo M, Ahlskog M and Stubb H 1992 *Synth. Met.* **48** 313
[59] Orgozall I, Lorenz B, Ting S T, Hor P H, Menon V, Martin C R and Hochheimer M D 1996 *Phys. Rev.* B **54** 16 654
[60] Jonscher A K 1983 *Dielectric Relaxation in Solids* (London: Chelsea Dielectric)
[61] Van Staveren M P J, Brom M B and de Jongh L J 1991 *Phys. Rep.* **208** 1
[62] Jonscher A K 1996 *Universal Relaxation Law* (London: Chelsea Dielectric)
[63] Davies M 1969 *Dielectric Properties and Molecular Behaviour* ed N E Hill, W E Vaughan, A H Price and M Davies (London: Van Nostrand Reinhold) p 285
[64] Hedvig P 1977 *Dielectric Spectroscopy of Polymers* (Bristol: Hilger)
[65] MacDonald J R 1987 *Impedance Spectroscopy* (New York: Wiley)
[66] McCrum N G, Read B E and Williams G 1967 *Anelastic and Dielectric Effects in Polymeric Solids* (New York: Dover)
[67] Summerfield S and Butcher P N 1984 *Phil. Mag.* B **49** L65
[68] Shimakawa K, Long A R and Inagawa O 1987 *Phil. Mag. Lett.* **56** 79
[69] Schroeder A, Pelster R, Grunow V, Lennartz W, Nimitz G and Friederich K 1996 *J. Appl. Phys.* **80** 2260
[70] Zuo F, Angelopoulos M, MacDiarmid A G and Epstein A J 1989 *Phys. Rev.* B **39** 3570
[71] Ping Sheng M, Xiaohua Q and Chune L 1993 *Synth. Met.* **55–57** 5008
[72] Lian A, Besner S and Dao L M 1995 *Synth. Met.* **74** 21
[73] Raghunathan A, Rangarajan G and Trivedi D C 1996 *Synth. Met.* **81** 39
[74] Kremer F, Rühe J and Meyer W H 1990 *Makromol. Chem. Macromol. Symp.* **37** 115
[75] Singh R, Tandon R P, Panwar V S and Chandra S 1991 *J. Appl. Phys.* **69** 2504
[76] Singh R, Tandon R P, Panwar V S and Chandra S 1991 *Thin Solid Films* **196** L15
[77] Singh R, Tandon R P, Panwar V S and Chandra S 1991 *J. Chem. Phys.* **95** 722
[78] Singh R, Narula A K, Tandon R P, Mansingh A and Chandra S 1996 *J. Appl. Phys.* **80** 985
[79] Singh R, Narula A K and Tandon R P 1996 *Synth. Met.* **82** 63
[80] Tanaka K, Nishio S, Masai K, Yamabe T and Yata S 1991 *Synth. Met.* **44** 35
[81] Chen S and Liao C 1993 *Synth. Met.* **55–57** 4936
[82] Chen S and Liao C 1993 *Synth. Met.* **60** 51
[83] Singh R and Narula A K 1996 *Synth. Met.* **82** 245